applied sciences

MDPI

Article

Proposal of Damage Index Ratio for Low- to Mid-Rise Reinforced Concrete Moment-Resisting Frame with Setback Subjected to Uniaxial Seismic Loading

Taufiq Ilham Maulana, Badamkhand Enkhtengis and Taiki Saito *

Department of Architecture and Civil Engineering, Toyohashi University of Technology, Aichi 441-8580, Japan; taufiq.ilham.maulana.mt@tut.jp (T.I.M.); badamkhand.enkhtengis.do@tut.jp (B.E.)
* Correspondence: saito.taiki.bv@tut.jp

Abstract: A vertical irregularity setback in reinforced concrete (RC) building affects its performance and response especially subjected to earthquake ground motions. It is necessary to understand how the seismic damage is established due to setbacks and avoid damage concentration on the irregularity section. The objective of this study is to propose a formula to estimate the damage distribution along the height of the setback building from a geometric measure of the degree of irregularity. First, previous experimental tests for two types of setback buildings, a towered and a stepped setback frames, were analyzed to verify the accuracy of the frame analysis. The results of the frame analysis considerably matched the experimental test results. Furthermore, to study the relationship between the degree of setback and the distribution of damage, a parametric study was conducted using 35 reinforced concrete setback frames, consisting of models with stepped setback type and towered setback type with different degrees of setback. The inelastic dynamic analyses of all the frames under three earthquake ground motions were conducted. The irregularity indices proposed in literature were adopted to express the degree of setback and the structural damage was expressed by the Park–Ang damage index. Using nonlinear regression analysis, formulas to estimate damage index ratio between two main structure parts (tower and base) from setback indices were proposed. Finally, the proposed formula was applied to the experimental test results to confirm its validity.

Keywords: setbacks; earthquake; damage index; seismic evaluation performance; damage distribution

check for updates

Citation: Maulana, T.I.; Enkhtengis, B.; Saito, T. Proposal of Damage Index Ratio for Low- to Mid-Rise Reinforced Concrete Moment-Resisting Frame with Setback Subjected to Uniaxial Seismic Loading. *Appl. Sci.* **2021**, *11*, 6754. https://doi.org/10.3390/app11156754

Academic Editor: Maria Favvata

Received: 9 June 2021
Accepted: 20 July 2021
Published: 22 July 2021

Publisher's Note: MDPI stays neutral with regard to jurisdictional claims in published maps and institutional affiliations.

Copyright: © 2021 by the authors. Licensee MDPI, Basel, Switzerland. This article is an open access article distributed under the terms and conditions of the Creative Commons Attribution (CC BY) license (https://creativecommons.org/licenses/by/4.0/).

1. Introduction

1.1. Background

In recent modern multistory building construction, the implementation of horizontal and vertical irregularities is getting popular due to different building functions and architectural needs. Vertical irregularity often regarded as a setback affects discontinuities in mass, stiffness, and structural strength distributions [1,2]. Under seismic excitations, this irregularity has a considerable effect on structure responses [3]. The existence of the setback may cause torsional response [4] and stress and damage concentration on the irregular part [5].

Studies on the seismic response of buildings with setbacks had been conducted by several researchers. Shakib and Pirizadeh [6] assessed the effect of simultaneous action of two orthogonal ground motion components on the performance of structure with different setback ratios and found that the effect of ground motion components is significant for the seismic performance of setback structures. Lin et al. [7] investigated the modal response history analysis of setback buildings and instead of using the conventional SDOF modal system, the 2DOF modal system was employed in modal response history analysis of building with specific vertical irregularities, to characterize the distinctly different modal response of tower and base structures. It was found that the 2DOF approach adequately captured the characteristic of drastic change in the peak interstory drift ratios between

tower and base. Georgoussis and Mamou [8] proposed the equations to minimize the rotational response due to the mass eccentricity of setback buildings by changing the location of lateral load resisting elements. The parameters in the proposed equations involved the first mode frequency and the displacement ratio between the tower and the base structure. The proposed equations were also applied for minimizing the rotational response of medium-rise buildings with irregular plans under seismic excitations [9].

Habibi and Asadi [10] developed equations to determine the Park–Ang damage index [11,12] of setback buildings using three independent parameters, namely overall drift (which is the ratio between the maximum roof displacement to the total height of the frame), the natural period, and the irregularity indices of the building. The adopted irregularity indices were originally introduced by Karavasilis et al. [13], involving the geometry of setback buildings, such as the number of stories and bays and the height and the width of setback buildings. Varadharajan et al. [14,15] also predicted the Park–Ang damage index of setback structures using three primary parameters: the ratio of modal participation factor between irregular and regular buildings, the beam to column stiffness ratio, and the displacement ductility. Hait et al. [16] assessed the Park–Ang damage index of low to mid-rise buildings using parameters generated from dynamic analyses, such as the maximum interstory drift, the peak roof displacement, and the maximum joint rotation of the members. Hait et al. [17]. also predicted the Park–Ang damage index by multi-variable regression using the artificial neural network. In these studies, the Park–Ang damage index was computed through nonlinear dynamic analysis for both tower and base sections, and the damage distribution could be retrieved after. This procedure could take time and resources for the dynamic analysis.

The objective of this paper is to propose the formula to determine the damage distribution of setback buildings based on the geometric measure of the degree of irregularity without conducting dynamic analysis. First, to verify the accuracy of the analytical method, the experimental tests for two types of setback buildings are analyzed. The experimental tests are a towered structure of fifteenth-scale 9-story 3-bay RC frame with a setback at level 3 by Wood [18] and a quarter model of 6-story 2-bay setback RC frame by Shahrooz and Moehle [19]. Then, the relationship between damage distribution of the Park–Ang damage index and the irregularity indices are examined by the parametric study of 35 models with different setback types. Finally, the nonlinear regression equations are proposed to determine the building damage distribution from the geometrical irregularity indices. Then, these equations are validated using the previous experimental results.

1.2. Park and Ang Damage Index

1.2.1. Definition

The damage index (DI) introduced by Park and Ang [11,12] is expressed by Equation (1). This DI value is based on the structural deformation and the hysteretic energy response due to seismic excitations.

$$DI = \frac{u_m}{u_u} + \beta \frac{E_h}{F_y u_u} \quad (1)$$

where:

u_m: Maximum displacement response of structure element due to earthquake,
u_u: Ultimate displacement capacity under a monotonic loading,
E_h: Hysteretic energy dissipated by the structural element,
F_y: Yield force,
β: Non-negative parameter based on repeated loading effect.

The relationship between the DI and the physical damage appearance for RC elements suggested by Park and Ang [12] is shown in Table 1. The parameters in Equation (1) are explained in the following passages.

Table 1. Damage Index for RC elements.

Damage Degree	Damage Index	Physical Appearance
Collapse	DI > 1.0	Collapse state
Severe	0.4 < DI < 1.0	Extensive crushing of concrete, disclosure of buckled reinforcement.
Moderate	0.25 < DI < 0.4	Extensive large cracks, spalling of concrete in weaker elements.
Minor	0.1 < DI < 0.25	Minor damage, light cracking throughout.
Slight	DI < 0.1	No damage or localized minor cracking

1.2.2. Determination of u_u

The ultimate displacement u_u is formulated as follows.

$$u_u = \mu_u u_y \tag{2}$$

where:

u_u: Ultimate displacement under monotonic loading,
μ_u: Ultimate ductility factor,
u_y: Yield displacement.

The yield displacement u_y is defined for each member based on element geometry and material properties. Due to the limitation of the available references stating clearly about the ultimate ductility factor μ_u, in this study, for each member, the μ_u is taken value as 15 by considering the probable failure mode occurs at the beam and column elements to be dominated as flexural failure [11].

1.2.3. Determination of β

The parameter β by Park and Ang [12] is presented in Equations (3) and (4).

$$\beta = (-0.447 + 0.073\frac{l}{d} + 0.24n_0 + 0.314p_t) \times 0.7^{p_w} \tag{3}$$

$$n_0 = \frac{N}{f_c bd} \tag{4}$$

where:

l/d: Shear span ratio (= 1.7 if l/d less than 1.7),
n_0: Normalized axial stress (= 0.2 if n_0 less than 0.2),
p_t: Longitudinal bars ratio, in percentage (= 0.75% if p_t less than 0.75%),
p_w: Transversal bars ratio,
N: Axial load,
f_c: Concrete compressive strength,
b: Width of cross section,
d: Effective height of cross section.

1.2.4. Damage Index of Building Component

The DI value is also suggested for a part of a structure, such as the individual story and the entire structure, by considering a weighting factor that is based on the dissipated hysteretic energy (E_h) of each member or the component as shown below, that are proposed originally by Park and Ang [12] and developed by Belkacem et al. [20]. Figure 1 shows the difference between DI_{story} and $DI_{component}$. In the component weighting factor calculation, the dissipated energy (E_h) considered is only in the same story, while the calculation of story weighting factor, all energies in all stories are considered.

$$DI_{Story} = \sum_{i=1}^{n_m} (\lambda_{i,component} DI_{i,component}) \tag{5}$$

$$\lambda_{i,component} = \left[\frac{E_{h,i}}{\sum_{i=1}^{n_m} E_{h,i}}\right]_{component} \quad (6)$$

$$DI_{overall} = \sum_{j=1}^{n_k} (\lambda_{j,story} DI_{j,story}) \quad (7)$$

$$\lambda_{j,story} = \left[\frac{E_{h,j}}{\sum_{j=1}^{n_k} E_{h,j}}\right]_{story} \quad (8)$$

where:

i: number of element member, starting at 1,
j: number of story, starting at 1,
n_k: total number of building's story,
n_m: total element member (beams and columns) in the reviewed story,
$DI_{i,component}$: Damage index for each component such as beam and column,
DI_{Story}: Damage index for each story,
$DI_{overall}$: Overall damage index,
$\lambda_{i,component}$: Weighting factor of each component,
$\lambda_{j,story}$: Weighting factor of each story.

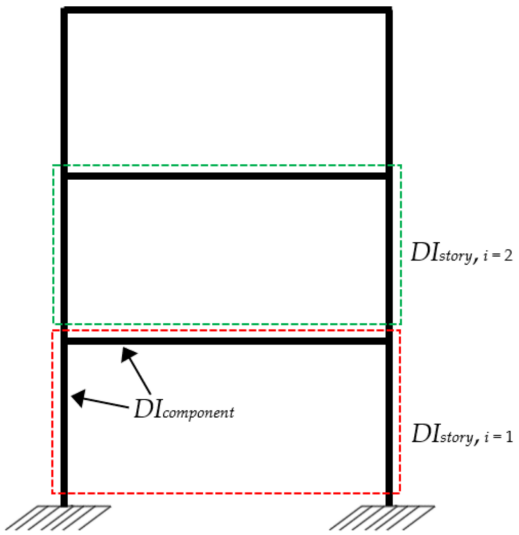


Figure 1. Illustration about damage index component and damage index story in a frame structure.

1.3. Setback Indices

Two kinds of vertical irregularities are selected to be studied: stepped and towered. The stepped type is a setback with the upper structure part at one side of the building, while the towered type is the condition when the upper structure part is in the middle region of the building. The illustration of the stepped type is shown in Figure 2a, and the towered type is shown in Figure 2b.

To consider the setback effect, two irregularity indices are adopted. These indices were initially introduced by Mazzolani and Piluso [21], which were then developed by Karavasilis et al. [13]. The indices describe the irregularity due to the presence of setbacks through simple geometrical indices φ_b and φ_s given by the following Equations (9) and (10).

$$\varphi_s = \frac{1}{n_s - 1} \times \sum_{i=1}^{i=n_s-1} \frac{L_i}{L_{i+1}} \quad (9)$$

$$\varphi_b = \frac{1}{n_b - 1} \times \sum_{i=1}^{i=n_b-1} \frac{H_i}{H_{i+1}} \tag{10}$$

where:

n_s: Number of stories of the frame,
n_b: Number of the bays of the first story of the frames,
H_i: Height of each bay from base to roof,
L_i: Total width of each story.

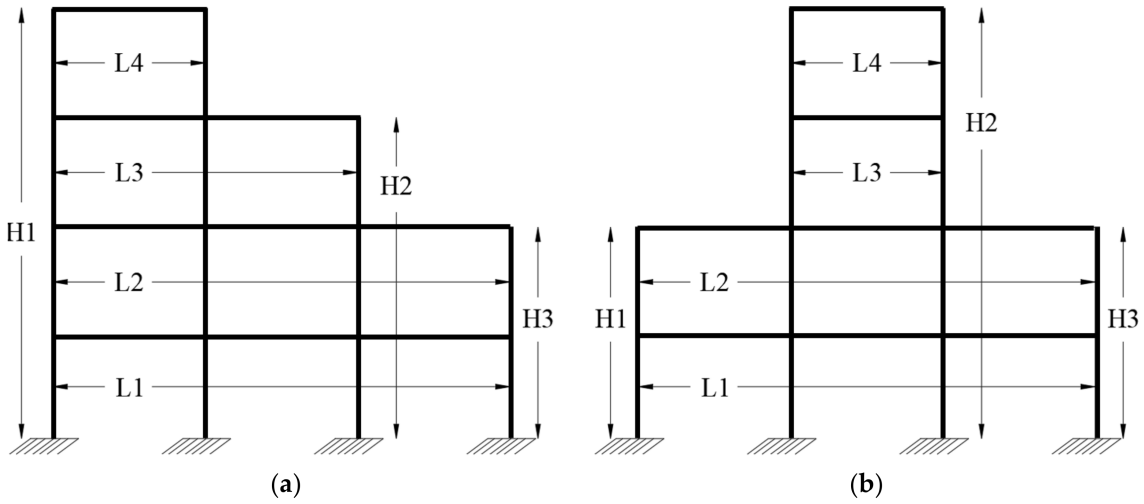


Figure 2. Frame geometry for irregularity indices definition for: (**a**) stepped type of setbacks; (**b**) towered type of setbacks.

In the case of stepped setback type, since the height H_i is counted from the left side, the value of φ_b will be different if the tower part is on the right side or on the left side. Therefore, in this study, H_i is always counted from the side that has the highest level.

2. Simulation of Setback RC Buildings Tested by Shaking Table

To verify the accuracy of the frame analysis, shaking table experimental tests of scaled setback RC buildings conducted by Wood in 1985 [18] and Shahrooz and Moehle in 1987 [19] were chosen to be numerically analyzed, and the raw data of both experimental tests were retrieved from DataCenterHub repository [22,23]. A software developed by one of the co-authors, STERA_3D, is used to perform the nonlinear dynamic structural analysis [24]. The following subchapters elaborate about the numerical tool and the detail of specimens.

2.1. Simulation Method of RC Frame Analysis

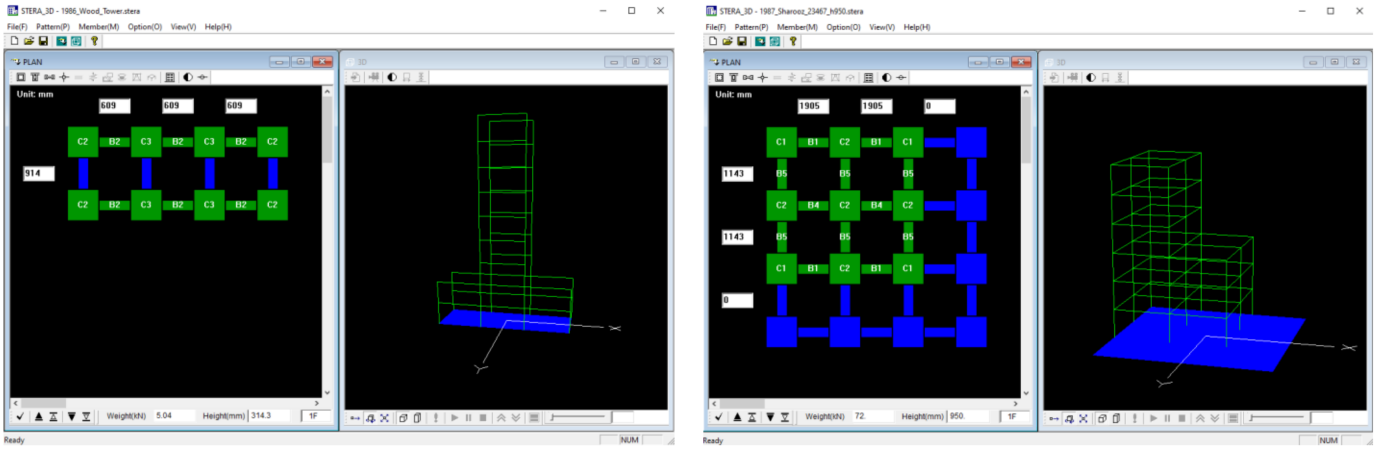
Figure 3a,b shows the interface of the STERA_3D for the test specimens of towered setback and stepped setback respectively. The RC beam element is modeled as a line element with two nonlinear flexural springs at both ends and one nonlinear shear spring at the middle as shown in Figure 4. The end displacement vector is obtained from Equation (11) as the sum of the displacement vector of each component. The dynamic earthquake response analysis is conducted by adopting Newmark-β numerical integration method [25].

$$\begin{Bmatrix} \theta_A \\ \theta_B \\ \delta_x \end{Bmatrix} = \begin{Bmatrix} \tau_A \\ \tau_B \\ \delta_x \end{Bmatrix} + \begin{Bmatrix} \varphi_A \\ \varphi_B \\ 0 \end{Bmatrix} + \begin{Bmatrix} \eta_A \\ \eta_B \\ 0 \end{Bmatrix} \tag{11}$$

where:

θ: the total rotation at the element joint,
δ_x: is the element deformation at direction x,

τ: is the elastic element rotation,
ϕ: is the nonlinear element rotation due to bending, and
η: is the nonlinear element rotation due to shear.



(**a**) (**b**)

Figure 3. STERA_3D interface on (**a**) a towered setback and (**b**) a stepped setback building models.

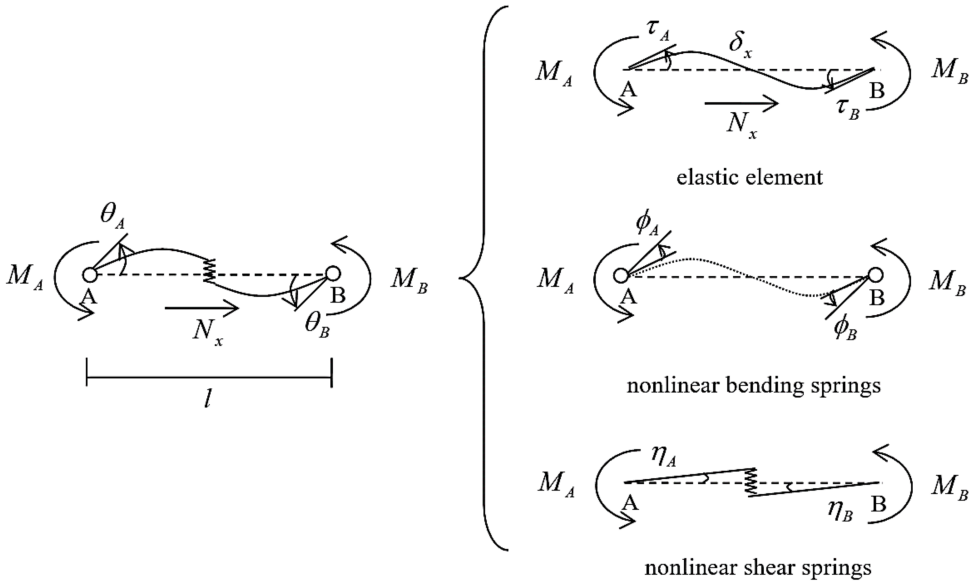


Figure 4. Elastic, nonlinear bending, and nonlinear shear springs for elements modeled by STERA_3D.

2.2. Simulation of Experimental Test of Towered Setback Structure

2.2.1. Specimen Description

The specimen tested by Wood [18] represents a scaled building with three bays and nine stories where the first story has a slightly higher elevation, and the setback location is in between level 2 and 3. The size of the experiment test frame model was 15 times smaller than the real building. The structure consists of two 2D beam-column frames, where the mass is attached to both frames using additional structures. For the first and second story, the weight is 5.04 kN, while the rest are 1.73 kN per level. The concrete compressive strength was 42.33 MPa, and the beam and column longitudinal rebar yielding strengths are 380.59 MPa and 388.17 MPa, respectively. The elevation of the specimen is presented in Figure 5.

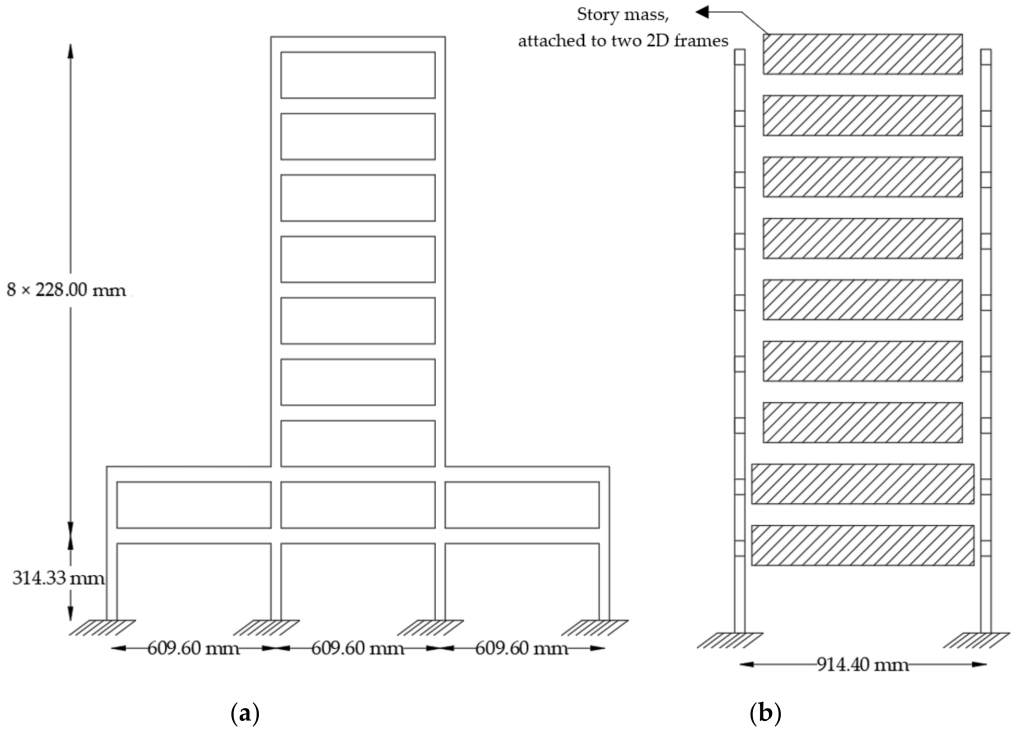


Figure 5. Experimental test specimen of towered setback structure: (**a**) front view, and (**b**) side view.

2.2.2. Input Data

For specimen of Wood [18], the input motion is only one direction parallel to the 2D frames. The input motions were a set of successive earthquake acceleration records, based on scaled 1940 El Centro NS with different magnitude. In this study, the first input of scaled 1940 El Centro NS with the peak acceleration of 382.8 cm/s^2 was used in the numerical study. The detail of input motion properties and the earthquake time history are presented in Table 2 and Figure 6.

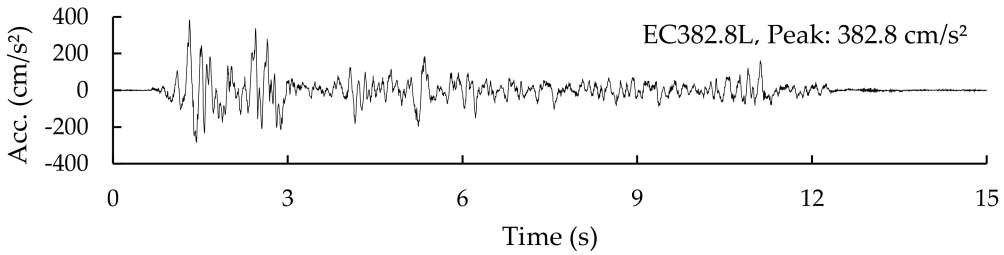


Figure 6. Time history acceleration of input motion.

Table 2. Detail of input motion properties.

No	Year	Event, Station	Component	Max. Acc. (cm/s^2)	Abbreviation	Input Direction
1	1940	scaled Imperial Valley, El Centro	NS	382.89	EC382.8L	Longitudinal

2.2.3. Results of Comparison

The maximum story drift and the maximum acceleration response of each story are shown in Figure 7a,b, and the time history of top floor displacement response is presented in Figure 8. Although there are some differences between analytical and experimental results, the trends of both displacement and acceleration responses are similar between simulation

and experiment. The demonstrated results show that STERA_3D software has the sufficient accuracy to conduct numerical dynamic analyses of towered setback structures.

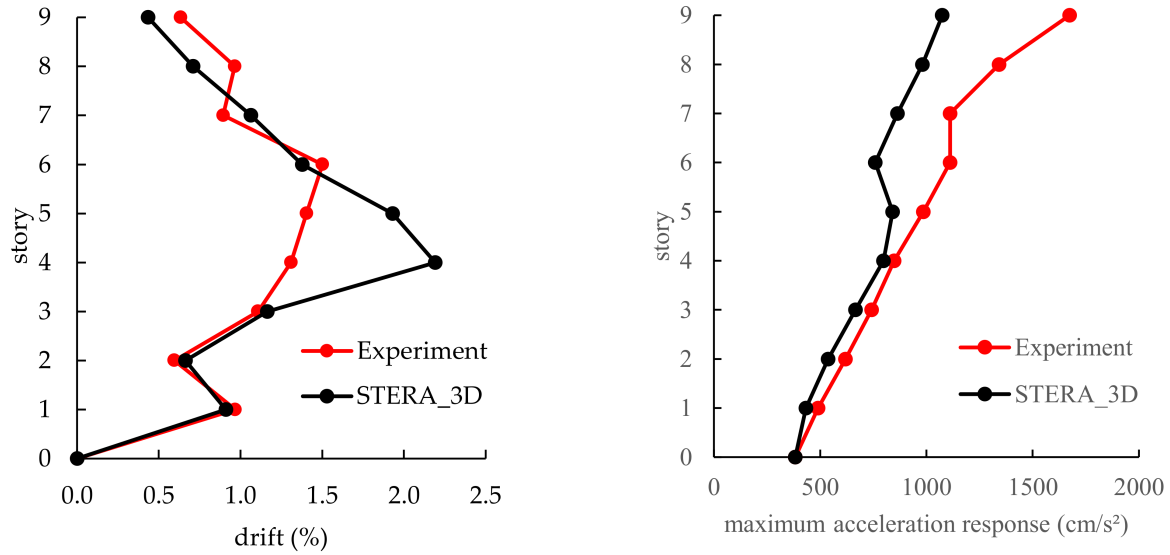


Figure 7. Comparison of experiment of towered setback structure with STERA_3D response: (**a**) interstory drift; (**b**) maximum acceleration.

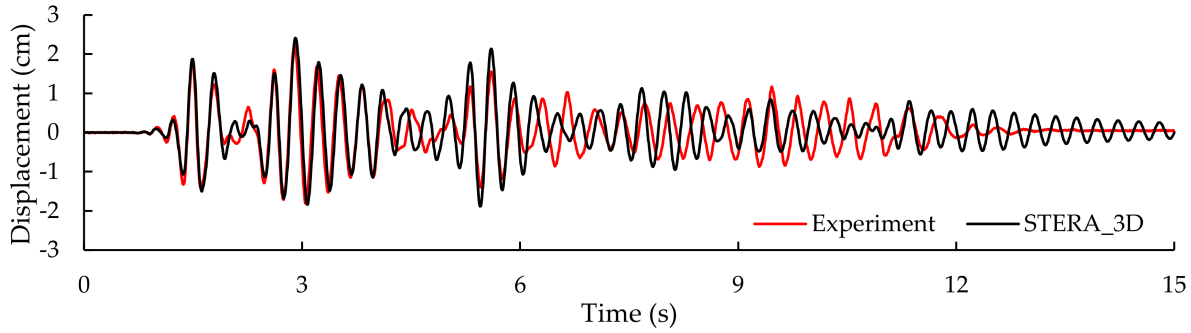


Figure 8. Roof displacement history responses of experiment of towered setback structure compared with STERA_3D.

2.3. Simulation of Experimental Test of Stepped Setback Structure

2.3.1. Specimen Description

The specimen tested by Shahrooz and Moehle [19] was designed for combined gravity and seismic effects according to the 1982 Uniform Building Code requirements to satisfy the seismic provisions of the American Concrete Institute Building Code (ACI 318-83) and the ACI-ASCE Committee 352 recommendations. The prototype is represented by the 1/4 scale model as depicted in Figure 9, in three dimensions with 2 2 bays of 1143 mm × 1905 mm floor panel size. Design concrete strength was 27.5 MPa, and all reinforcement was Grade 60 (minimum yield stress of 413 MPa). The weight of structures is 72 kN per level for first to third story and 41 kN per level for fourth to sixth story, and the inter story height is 914.4 mm.

2.3.2. Input Data

The specimen of Shahrooz and Moehle [19] was subjected to two input motions sequentially: unidirectional and bidirectional. The first stage consists of three different scaled 1940 El Centro NS ground motions, while the second phase includes three unidirectional horizontal motions inputted at an angle of 45 degrees to simulate bidirectional motions.

In this study, the numerical analysis only focuses on the longitudinal study and neglects the bidirectional simulation. The detail of input motion properties and the earthquake time histories are presented in Table 3 and Figure 10.

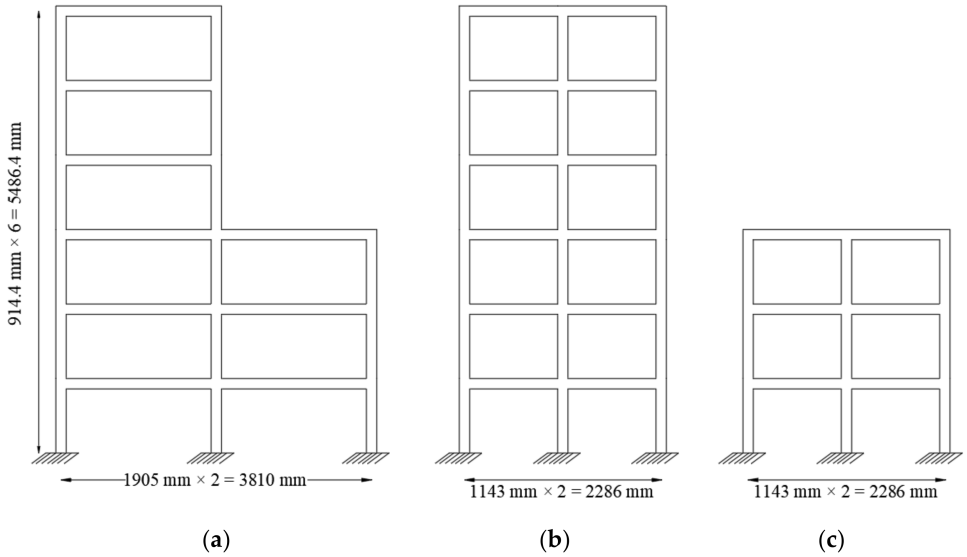


Figure 9. Elevation view of setback experimental test specimen: (**a**) front view, (**b**) side left view, and (**c**) side right view.

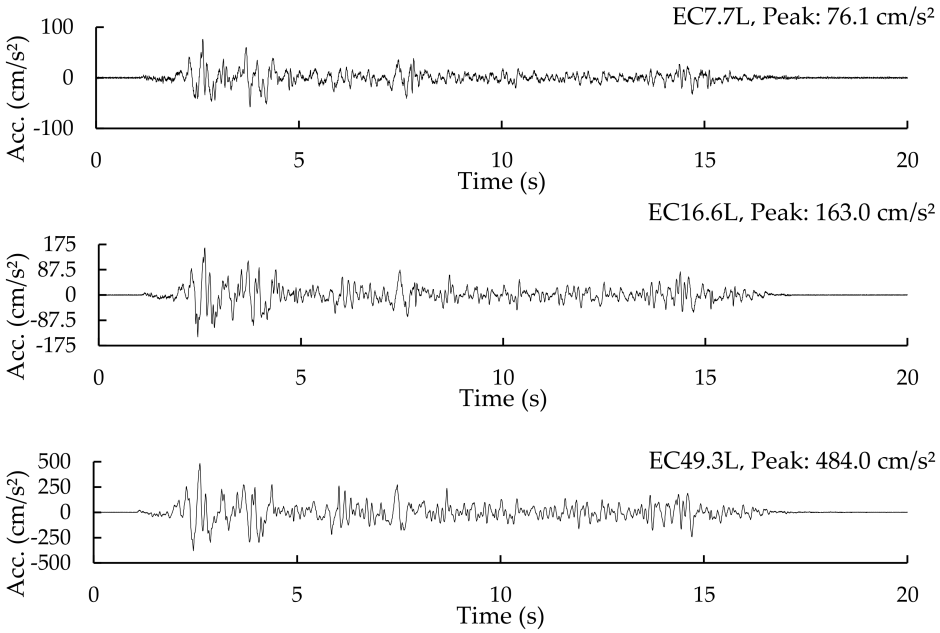


Figure 10. Time history acceleration of input motions.

Table 3. Detail of input motion properties.

No	Year	Event, Station	Component	Max. Acc. (cm/s^2)	Abbreviation	Input Direction
1	1940	scaled Imperial Valley, El Centro	NS	76.10	EC7.7L	Longitudinal
2				163.00	EC16.6L	
3				484.00	EC49.3L	

2.3.3. Results of Comparison

The relative maximum displacement response and the absolute maximum acceleration response of unidirectional experimental tests by Shahrooz and Moehle [19] and analytical tests are depicted in Figure 11a,b, and the time history of displacement response at the top floor against the last input motion is presented in Figure 12. The result shows that there are only slight differences between experiment and simulation in both acceleration and displacement response.

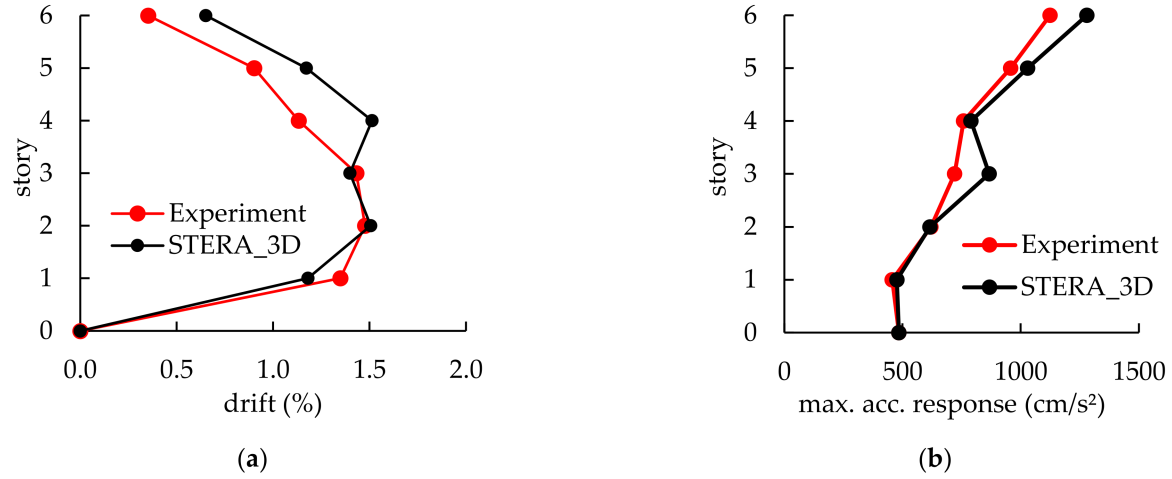


Figure 11. Comparison of experiment of stepped setback structure specimen with STERA_3D response: (**a**) interstory drift; (**b**) maximum acceleration.

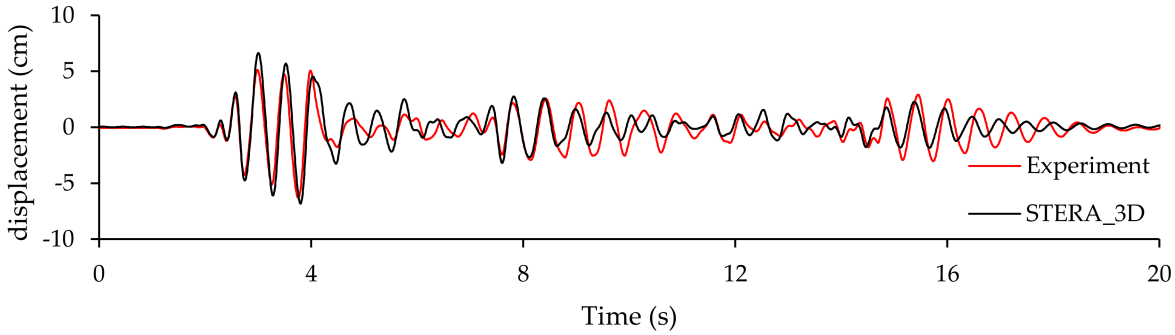


Figure 12. Roof displacement history responses of experiment of stepped setback structure compared with STERA_3D.

3. Parametric Study of Generated Setback Frames

To examine the relationship between the degree of setback and the distribution of damage, a parametric study was conducted using 35 reinforced concrete setback frames, consisting of 20 models with stepped setback type and 15 models with towered setback type with different degree of setback as depicted in Figures 13 and 14. All the frames have six stores with the number of bays ranging from two to five depending on the model. Each of generated models is represented with two numbers at the above frame illustration. The first number is the difference of the number of bays between top and base structures and the second number is the number of stories in the top structure.

The typical plan of the structure is shown in Figure 15. All the frames use one type of beam section, namely B1, and one type of column section, namely C1. The concrete compressive strength is 30 MPa, while the yield strength of both longitudinal and transversal rebars are 390 MPa. The slab thickness is 15 cm with reinforcement of D13 with the spacing of 10 cm. The section details of elements are presented in Table 4. The total gravity load implemented for every floor is 12 kN/m^2.

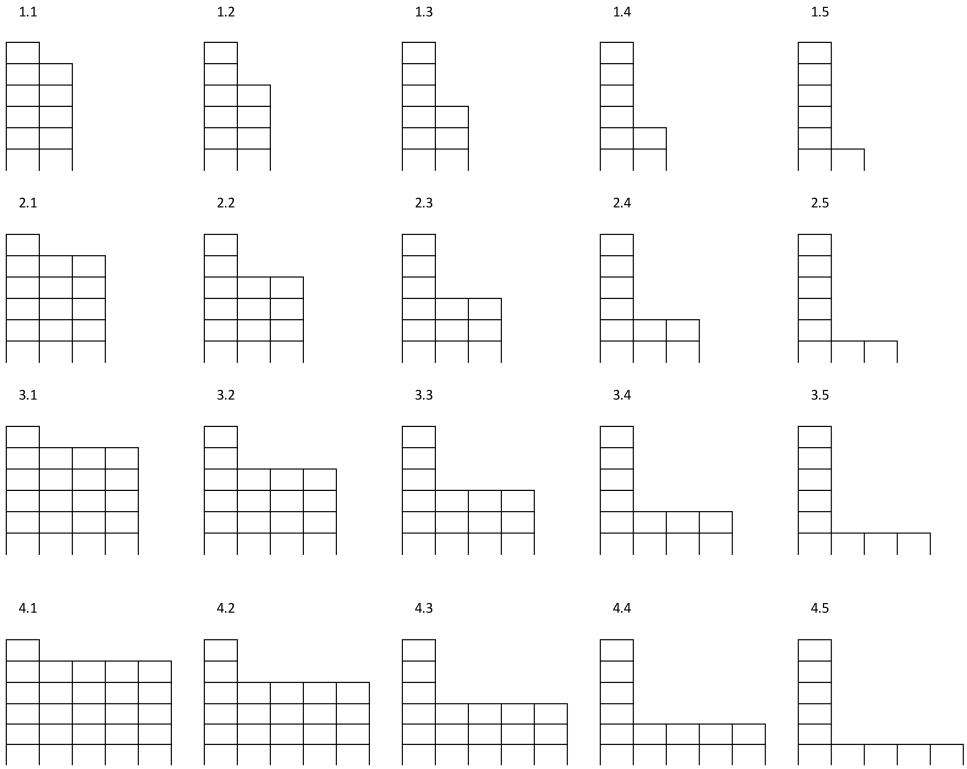


Figure 13. Generic 2D frame structures of stepped setback model.

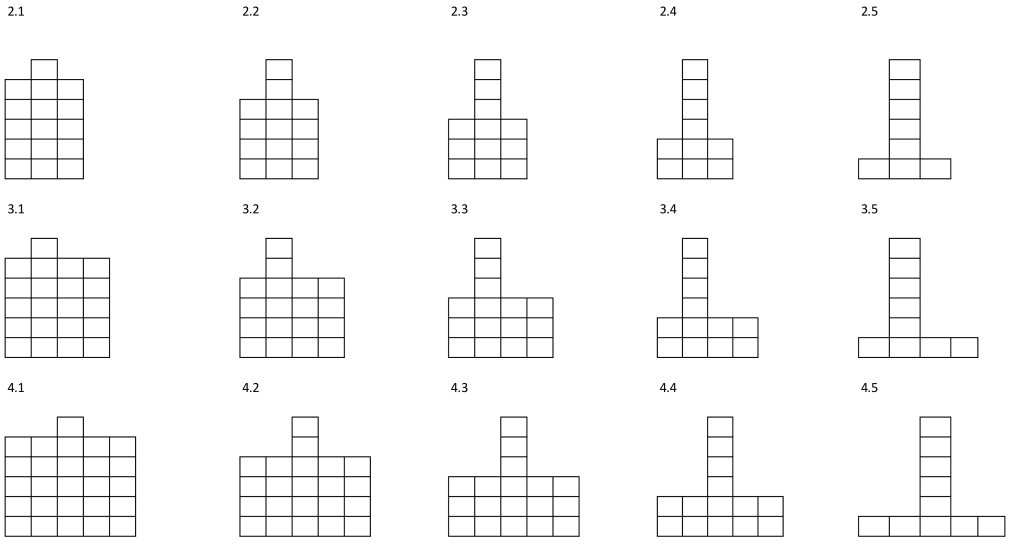


Figure 14. Generic frame structures of towered setback model.

Table 4. Section details of column and beam.

No	Element	Code	Story Level	Depth (mm)	Width (mm)	Longitudinal Rebars	Transversal Rebars
1	Column	C1	1–6	700	700	8 D-35	2 D-13 @ 10 cm
2	Beam	B1	1–6	600	300	3 D-35 on top and 3 D-35 on bottom	2 D-13 @ 15 cm

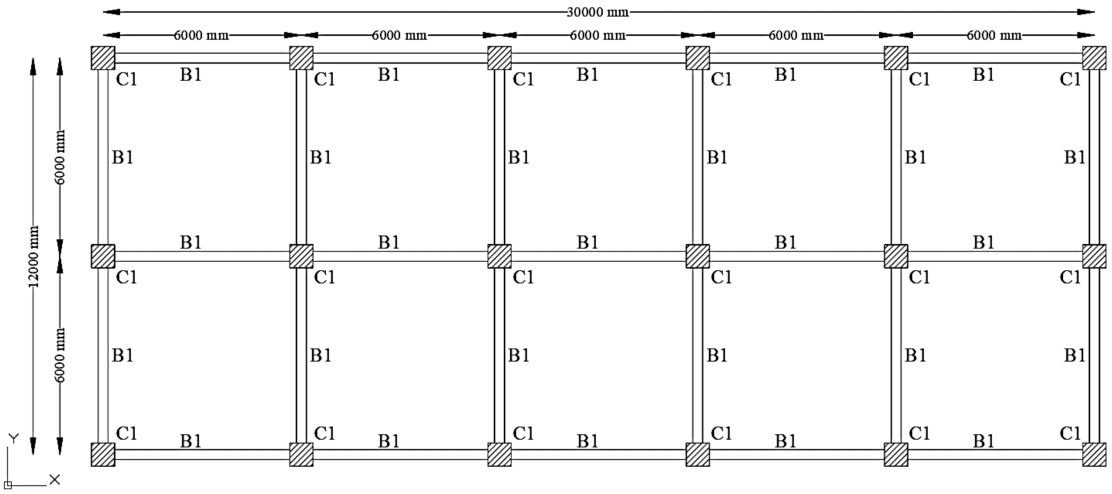


Figure 15. 2D plan of generated structure of 2 × 5 bays for 6-story building.

Nonlinear dynamic analyses were performed using STERA_3D, and the story damage indices were populated. The list of input earthquake ground motions is shown in Table 5. Ten input ground motions are recorded acceleration waves scaled to have the maximum velocity of 50 cm/s. The ground motion data are retrieved from PEER [26] and COSMOS Virtual Data Center [27]. The intensity of these input ground motions corresponds to the level of design earthquakes for the safety limit state in the Japanese seismic standard. The acceleration response spectrum is presented in Figure 16, and the wave shapes of the earthquake input motions are depicted in Figure 17.

Table 5. Selected earthquake ground motion.

No	Event	Year	Station	Component	Original Max. Acc. (cm/s^2)	Scaled Max. Acc. (cm/s^2)
1	Imperial Valley	1940	El Centro	NS	341.69	510.70
2	Kern County	1952	Taft	EW	152.69	496.50
3	Chi-chi	1999	CHY080	360 DEG	836.84	434.04
4	Northridge	1994	Arleta-Nordhoff Ave Fire Station	90 DEG	337.32	417.87
5	Loma Prieta	1989	Saratoga-Aloha Ave	0 DEG	494.45	597.96
6	Valparaiso, Chile	1985	Vina del Mar	200 DEG	355.50	578.31
7	Villita, Mexico	1985	Guerrero Array Stn VIL	N00W	125.37	318.36
8	Cape Mendocino	1992	Petrolia	0 DEG	578.14	598.43
9	Cape Mendocino	1992	Rio Dell-101/Painter St. Overpass	270 DEG	378.27	422.98
10	Kobe	1995	JMA	NS	817.80	449.80

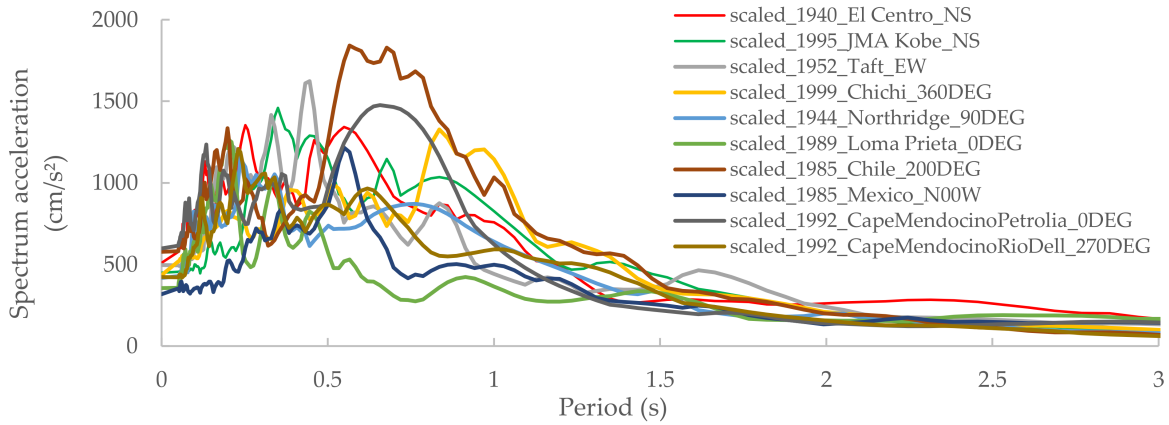


Figure 16. Acceleration response spectra (with 5% damping factor) of input earthquake motions.

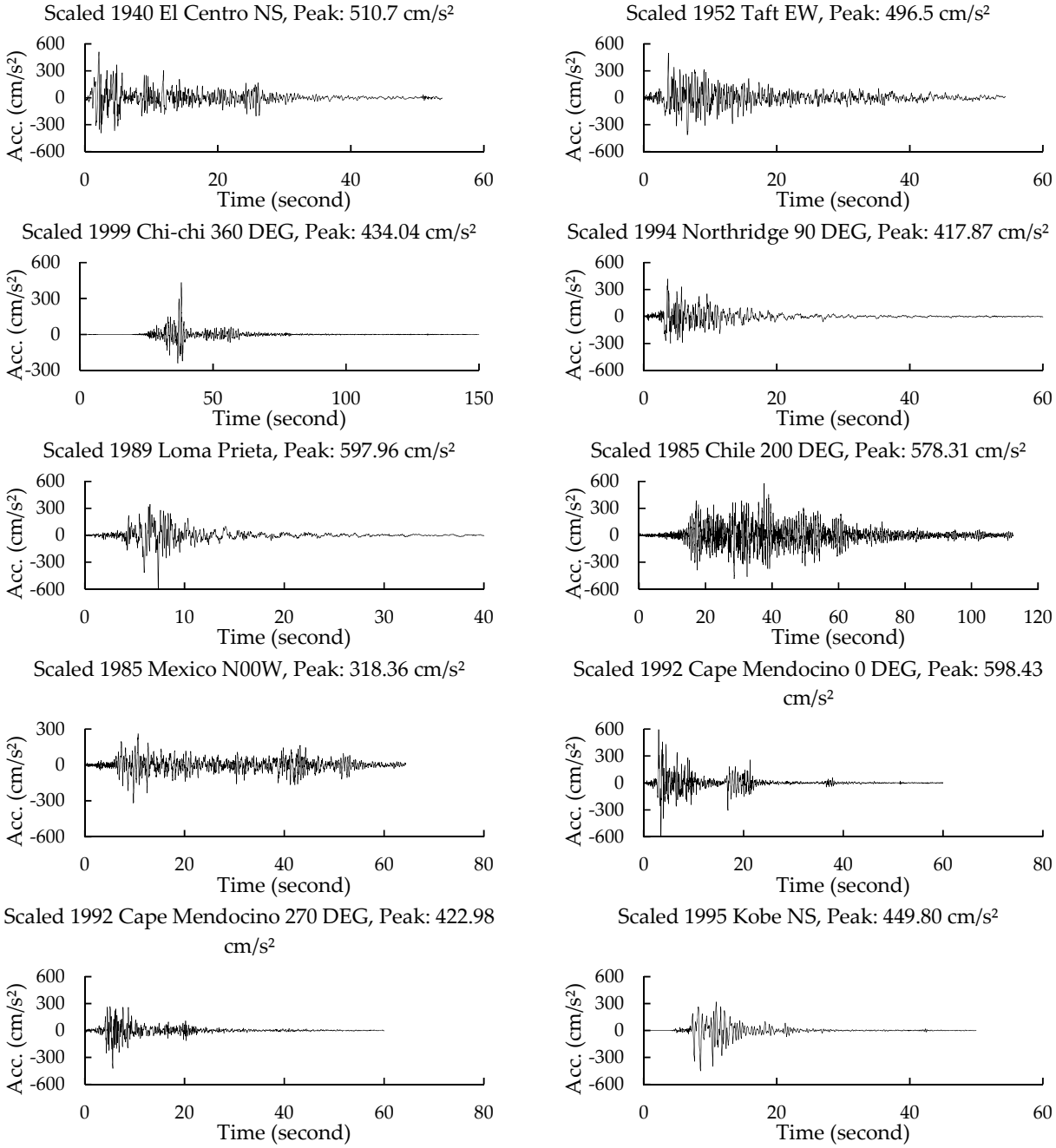


Figure 17. Time history acceleration waves of input earthquake motions.

4. Proposal of Tower-Base Damage Index Ratio

The nonlinear dynamic analysis using STERA_3D was conducted for all 35 frames with three input earthquake ground motions to calculate the damage index (*DI*) of each story. The damage index of each story is calculated using Equation (5). The following DI_{ratio} is proposed to examine the distribution of the *DI* along the height of the frame.

$$DI_{ratio} = \frac{\max(DI_{tower})}{\max(DI_{base})} \tag{12}$$

where the DI_{tower} and DI_{base} are taken as the average for the ten input ground motions. If the value of DI_{ratio} is larger than one, the damage will be concentrated at the tower structure. Conversely, if the value is less than one, the base structure will suffer more damage than the tower.

The mathematical model is developed for predicting DI_{ratio} from irregularity indices φ_s and φ_b using the nonlinear regression analysis so that the damage distribution is easily evaluated without conducting the nonlinear dynamic analysis. The relation between the calculated DI_{ratio} of all the frames and irregularity indices φ_s and φ_b are shown in Figure 18 for the stepped model and Figure 19 for the towered model type, respectively.

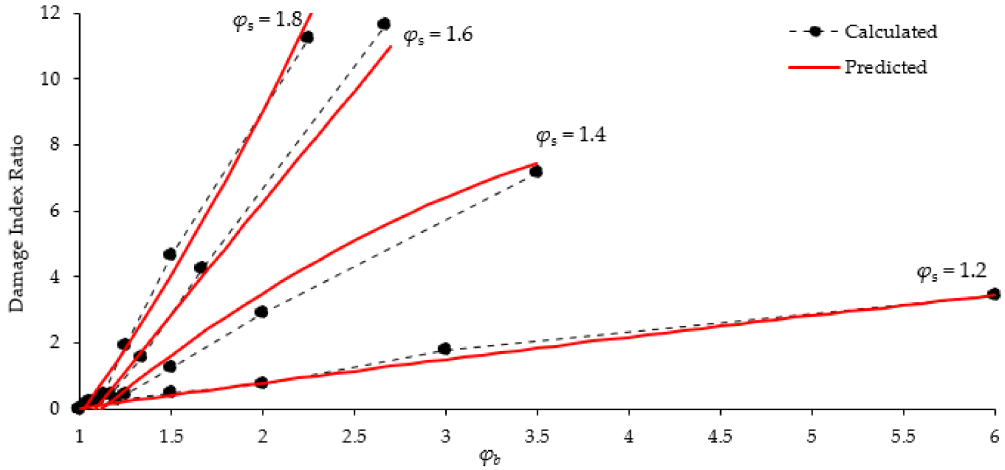


Figure 18. DI_{ratio} with different φ_s and φ_b for stepped model.

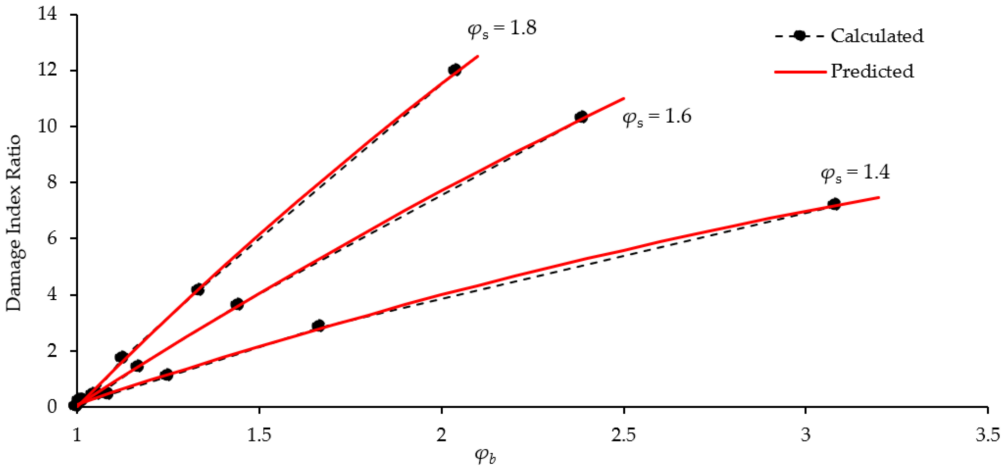


Figure 19. DI_{ratio} with different φ_s and φ_b for towered model.

Values of φ_s and φ_b equal to 1 correspond to a structure with a uniform configuration. As values of φ_s and φ_b increase, the degree of the setback in the frame structure becomes larger. A large value of DI_{ratio} indicates a relatively large damage concentration in the tower. The nonlinear regression analysis is performed to derive the quadratic polynomial equation for estimating the damage index ratios from irregularity indices,φ_s and φ_b. The obtained equations are shown in Equation (13) for stepped type and Equation (14) for towered type. The red lines in Figures 18 and 19 indicate the prediction of the damage index ratio using Equations (13) and (14). The values of R-squared of red lines, which indicate the goodness-of-fit measure for the regression model, vary between 0.865 and 0.999.

$$DI_{r,stepped} = 98.19 - 124.29\varphi_s - 105.06\varphi_b + 142.75\varphi_s\varphi_b + 38.34{\varphi_s}^2 + 25.47{\varphi_b}^2 - 37.09\varphi_s{\varphi_b}^2 - 45.44{\varphi_s}^2\varphi_b + 13.22{\varphi_s}^2{\varphi_b}^2 \quad (13)$$

$$DI_{r,towered} = -3.09 + 16.89\varphi_s + 17.22\varphi_b - 35.99\varphi_s\varphi_b - 12.88{\varphi_s}^2 - 12.53{\varphi_b}^2 + 17.34\varphi_s{\varphi_b}^2 + 19.59{\varphi_s}^2\varphi_b - 6.22{\varphi_s}^2{\varphi_b}^2 \quad (14)$$

5. Validation of Proposed Damage Index Ratio

To validate the proposed method to calculate DI_{ratio}, the towered setback frame by Wood [18] and the stepped setback frame tested by Shahrooz and Moehle [19] are examined. The input wave is the 1940 El Centro NS record scaled to have the maximum velocity of 50 cm/s; however, the time step is adapted for each specimen. The specimen of Wood [18] is subjected to the earthquake with the time step divided by 4 by rounding up the value of $\sqrt{15}$, while the specimen of Shahrooz and Moehle [19] is subjected to the earthquake with the time step divided by 2, by considering the scale factor of test specimen. Dynamic time history analysis was performed using STERA_3D to calculate the *DI* of each story. The calculated damage index ratios were compared with the predicted damage index ratios from the proposed equations and presented in Table 6.

Table 6. Numerical analysis result compared to prediction result using Regression Equation.

Frame	φ_b	φ_s	Natural Period T (s)	Calculated DI_{ratio}	Predicted DI_{ratio}	Accuracy (%)
Wood [18]	2.75	1.25	0.118	1.2691	1.3552	93.22
Shahrooz and Moehle [19]	2.00	1.20	0.248	1.1641	0.7766	66.71

The accuracy of the prediction from Equation (13) is adequate, 66% for the stepped setback and the prediction accuracy from Equation (14) is relatively high, 93% for the towered setback.

6. Conclusions

To understand better the earthquake response and damage concentration of setback buildings, numerical investigations were conducted and a practical method to evaluate the damage distribution was proposed.

First, two previous experimental tests of reinforced concrete buildings comprising a towered setback and a stepped setback were modeled and analyzed by STERA_3D and the test results were successfully simulated.

Then, to study the building damage distribution, 2D reinforced concrete frame models containing 20 stepped and 15 towered setback frames were generated to inspect the relationship between the damage index ratio and the irregularity indices under safety level earthquake input ground motions. Based on the results, two nonlinear regression equations were proposed as an alternative to the dynamic analysis procedures.

Finally, the proposed equations were applied to the previous experimental tests, and it was demonstrated that the proposed formulas could predict the damage to vertically irregular reinforced concrete moment-resisting frame with reasonable accuracy. Although the prediction formula works, it is important to be noted that the setback buildings considered in this study are limited for low- to mid-rise reinforced concrete frame buildings with uniaxial seismic loading.

Author Contributions: Conceptualization, T.S., B.E. and T.I.M.; methodology, B.E., T.I.M.; software, T.S.; writing—original draft preparation, T.I.M.; writing—review and editing, T.S.; supervision, T.S. All authors have read and agreed to the published version of the manuscript.

Funding: This research received no external funding.

Institutional Review Board Statement: Not applicable.

Informed Consent Statement: Not applicable.

Data Availability Statement: The data presented in this study are available on request from the corresponding author.

Acknowledgments: The first author appreciates AUN/SEED-Net JICA for the support through scholarship of doctoral degree.

Conflicts of Interest: The authors declare no conflict of interest.

References

1. Soni, D.P.; Mistry, B.B. Qualitative review of seismic response of vertically irregular building frames. *ISET J. Earthq. Technol.* **2006**, *43*, 121–132.
2. Mwafy, A.; Khalifa, S. Effect of vertical structural irregularity on seismic design of tall buildings. *Struct. Des. Tall. Spec. Build.* **2017**, *26*, 1–22. [CrossRef]
3. Shahrooz, B.M.; Moehle, J.P. Seismic response and design of setback buildings. *J. Struct. Eng.* **1990**, *116*, 1423–1439. [CrossRef]
4. Duan, X.N.; Chandler, A.M. Seismic torsional response and design procedures for a class of setback frame buildings. *Earthq. Eng. Struct. Dyn.* **1995**, *24*, 761–777. [CrossRef]
5. Dutta, S.C.; Das, P.K.; Sengupta, P. Seismic behaviour of irregular structures. *Struct. Eng. Int.* **2017**, *27*, 526–545. [CrossRef]
6. Shakib, H.; Pirizadeh, M. Probabilistic seismic performance assessment of setback buildings under bidirectional excitation. *J. Struct. Eng.* **2014**, *140*, 04013061. [CrossRef]
7. Lin, J.-L.; Tsaur, C.-C.; Tsai, K.-C. Two-degree-of-freedom modal response history analysis of buildings with specific vertical irregularities. *Eng. Struct.* **2019**, *184*, 505–523. [CrossRef]
8. Georgoussis, G.K.; Mamou, A. Mitigating mass eccentricity effects on the rotational response of setbacks structures: An analytical solution for linear systems. *Structures* **2020**, *28*, 1539–1556. [CrossRef]
9. Georgoussis, G.K. An approach for minimum rotational response of medium-rise asymmetric structures under seismic excitations. *Adv. Struct. Eng.* **2016**, *19*, 420–436. [CrossRef]
10. Habibi, A.; Asadi, K. Development of drift-based damage index for reinforced concrete moment resisting frames with setback. *Int. J. Civ. Eng.* **2017**, *15*, 487–498. [CrossRef]
11. Park, Y.-J.; Ang, A.H.-S. Mechanistic seismic damage model for reinforced concrete. *J. Struct. Eng.* **1985**, *111*, 722–739. [CrossRef]
12. Park, Y.-J.; Ang, A.H.-S.; Wen, Y.K. Seismic damage analysis of reinforced concrete buildings. *J. Struct. Eng.* **1985**, *111*, 740–757. [CrossRef]
13. Karavasilis, T.L.; Bazeos, N.; Beskos, D.E. Seismic response of plane steel MRF with setbacks: Estimation of inelastic deformation demands. *J. Constr. Steel Res.* **2008**, *64*, 644–654. [CrossRef]
14. Varadharajan, S.; Sehgal, V.K.; Saini, B. Determination of inelastic seismic demands of RC moment resisting setback frames. *Arch. Civ. Mech. Eng.* **2013**, *13*, 370–393. [CrossRef]
15. Varadharajan, S.; Sehgal, V.K.; Saini, B. Seismic behavior of multistory RC building frames with vertical setback irregularity. *Struct. Des. Tall. Spec. Build.* **2014**, *23*, 1345–1380. [CrossRef]
16. Hait, P.; Sil, A.; Choudhury, S. Damage assessment of low to mid rise reinforced concrete buildings considering planner irregularities. Int. J. Comput. *Methods Eng. Sci. Mech.* **2020**, *22*, 150–168.
17. Hait, P.; Sil, A.; Choudhury, S. Seismic damage assessment and prediction using artificial neural network of RC building considering irregularities. *Int. J. Struct. Integr. Maint.* **2020**, *5*, 51–69. [CrossRef]
18. Wood, S.L. Experiments to Study the Earthquake Response of Reinforced Concrete Frames with Setbacks. Ph.D. Thesis, University of Illinois at Urbana-Champaign, Champaign, IL, USA, 1985.
19. Shahrooz, B.M.; Moehle, J.P. *Experimental Study of Seismic Response of RC Setback Buildings*; National Science Foundation Report; UCB: Berkeley, CA, USA, 1987.
20. Belkacem, M.A.; Bechtoula, H.; Bourahla, N.; Belkacem, A.A. Damage index for reinforced concrete columns. *Građevinar* **2020**, *72*, 139–149.
21. Mazzolani, F.; Piluso, V. *Theory and Design of Seismic Resistant Steel Frames*; E & FN Spon: London, UK, 1996.
22. Shahrooz, B.M.; Moehle, J.P. Experimental Study of Seismic Response of Reinforced Concrete Setback Buildings. Available online: https://datacenterhub.org/deedsdv/publications/view/293 (accessed on 1 October 2020).
23. Wood, S.L.; Sozen, M. Experiments to Study the Earthquake Response of Reinforced Concrete Frames with Setbacks (NEES-2011-1068). Available online: https://datacenterhub.org/deedsdv/publications/view/285 (accessed on 1 October 2020).
24. Saito, T. Structural Earthquake Response Analysis, STERA_3D Version 10.8. Available online: http://www.rc.ace.tut.ac.jp/saito/software-e.html (accessed on 1 October 2020).
25. Newmark, N.M. A method for computation of structural dynamics. *J. Eng. Mech. Div.* **1959**, *85*, 67–94. [CrossRef]
26. PEER (Pacific Earthquake Engineering Center). Ground Motion Database. Available online: https://peer.berkeley.edu/ (accessed on 4 July 2021).
27. COSMOS (The Consortium of Organizations for Strong-Motion Observation Systems). Virtual Data Center. Available online: www.strongmotioncenter.org (accessed on 4 July 2021).